

Low heat conduction in white dwarf boundary layers?

F. K. Liu¹, F. Meyer², E. Meyer-Hofmeister², and V. Burwitz³

¹ Astronomy Department, Peking University, Beijing 100871, PR China
e-mail: fkliau@pku.edu.cn

² Max-Planck-Institut für Astrophysik, Karl-Schwarzschildstr. 1, 85740 Garching, Germany
e-mail: [frm;emm]@mpa-garching.mpg.de

³ Max-Planck-Institut für extraterrestrische Physik, PO Box 1312, 85741 Garching, Germany
e-mail: burwitz@mpe.mpg.de

Received 17 December 2007 / Accepted 17 February 2008

ABSTRACT

Context. X-ray spectra of dwarf novae in quiescence observed by Chandra and XMM-Newton provide new information on the boundary layers of their accreting white dwarfs.

Aims. Comparison of observations and models allows us to extract estimates for the thermal conductivity in the accretion layer and reach conclusions on the relevant physical processes.

Methods. We calculate the structure of the dense thermal boundary layer that forms under gravity and cooling at the white dwarf surface on accretion of gas from a hot tenuous ADAF-type coronal inflow. The distribution of density and temperature obtained allows us to calculate the strength and spectrum of the emitted X-ray radiation. They depend strongly on the values of thermal conductivity and mass accretion rate.

Results. We apply our model to the dwarf nova system VW Hyi and compare the spectra predicted for different values of the thermal conductivity with the observed spectrum. We find a significant deviation for all values of thermal conductivity that are a sizable fraction of the Spitzer conductivity. A good fit arises however for a conductivity of about 1% of the Spitzer value. This also seems to hold for other dwarf nova systems in quiescence. We compare this result with thermal conduction in other astrophysical situations.

Conclusions. The highly reduced thermal conductivity in the boundary layer requires magnetic fields perpendicular to the temperature gradient. Locating their origin in the accretion of magnetic fields from the hot ADAF-type coronal flow we find that dynamical effects of these fields will lead to a spatially intermittent, localized accretion geometry at the white dwarf surface.

Key words. stars: dwarf novae – accretion, accretion disks – X-rays: individuals: VW Hyi – conduction – magnetic fields – galaxies: cooling flows

1. Introduction

Cataclysmic variables (CVs) are interacting binaries in which mass flows from a low mass companion star and accretes on the white dwarf primary. The X-ray emission of the large number of cataclysmic variables makes up a large fraction of the apparently diffuse Galactic Ridge X-ray emission, as was recently found with the help of deep surveys by *Chandra* and *XMM-Newton* (Sazonov et al. 2006). In dwarf nova systems, non-magnetic CVs, the accretion onto the white dwarf occurs via an accretion disk and the gas must dissipate its rotational kinetic energy before it settles on the surface of the more slowly rotating white dwarf. The X-ray emission is thought to originate from the interface between the white dwarf and the inner edge of the disk, a boundary layer close to the surface. The disk is too cool to contribute significantly to the X-ray emission.

Different models have been proposed for the structure of the X-ray emitting region in dwarf nova at low accretion rates, i.e. in their quiescent state: (1) a cooling flow model based on Mushotzky & Szymkowiak (1988), which assumes isobaric radiative cooling of the gas; (2) a model of a hot boundary layer where heat advection is dominant (Narayan & Popham 1993); (3) a thermal boundary layer model where heat conduction determines the structure of the spherically accreting gas around the white dwarf (Liu et al. 1995) and a similar X-ray emitting corona model of Mahasena & Osaki (1999); and (4) hot settling flow so-

lutions (Narayan & Medvedev 2001; Medvedev & Menou 2002) in which viscously mediated losses of rotational energy are an important parameter. In these papers references to earlier discussions of emission mechanisms are given.

The much improved sensitivity and spectral resolution of the new X-ray telescopes allow us to test specific models. The first tests were performed by Pandel et al. (2003) for VW Hyi in quiescence and by Perna et al. (2003) for WX Hydri in quiescence. Pandel et al. (2003) used X-ray and ultraviolet data obtained with *XMM-Newton*. The authors found that the X-ray spectrum indicates the presence of optically thin plasma in the boundary layer that cools as it settles on the white dwarf, and that the plasma has a range of temperatures that is well described by a power law or a cooling flow model with a maximum temperature of 6–8 keV. Perna et al. (2003) used *Chandra* observations for their investigation, computed spectra for the available theoretical models, i.e. hot boundary layers, hot settling flows and X-ray emitting coronae. They came to the conclusion that the continuum is reproduced well by most of the models, but none of them can fully account for the relative line strengths over the entire spectral range. Pandel et al. (2005) studied 10 dwarf novae, based on *XMM-Newton* observations, including the earlier results for VW Hyi by Pandel et al. (2003). The authors conclude that the X-ray emission originates from a hot, optically thin multi-temperature plasma with a temperature distribution

1 in close agreement with an isobaric cooling flow, pointing to a
2 cooling plasma settling onto the white dwarf as the source of
3 X-rays.

4 We use the model description worked out earlier (Liu et al.
5 1995), which is related to the “siphon flow model” for a
6 corona above an accretion disk in quiescence (Meyer & Meyer-
7 Hofmeister 1994). In this picture matter in the innermost disk
8 is evaporated into a coronal flow which provides a geometri-
9 cally thick gas flow towards and around the white dwarf. (Dwarf
10 nova systems have cycles of longer lasting quiescent phases and
11 shorter outbursts. These outbursts are triggered by a disk insta-
12 bility, then the matter accumulated in the disk during quiescence
13 accretes with a high mass flow rate onto the white dwarf Meyer
14 & Meyer-Hofmeister (1984). For the formation of the inner disk
15 hole see Liu et al. 1997). Since the flow of gas from the surround-
16 ing corona is an essential feature of our model our approach dif-
17 fers from the simulation of the boundary layer between a white
18 dwarf and a thin accretion disk which extends all the way down
19 to the stellar surface, as studied recently by Balsara et al. (2007).
20 These numerical simulations give insight into the spreading of
21 the boundary layer, but no conclusions on spectra are derived.

22 We have chosen the well documented dwarf nova VW Hyi
23 for our new investigation. We compute the thermal boundary
24 layer structure, evaluate the emission measures and determine
25 spectra using the XSPEC package. We come to the somewhat
26 surprising result that only structures based on very low conduc-
27 tivity give spectra in agreement with the observations. Pandel
28 et al. (2005) already remarked that heat conduction does not
29 dominate over cooling via X-ray emission because otherwise
30 T_{\max} , the initial temperature of the cooling gas, would be much
31 smaller than the virial temperature T_{vir} (the temperature the gas
32 would have if all the rotational energy from its Keplerian mo-
33 tion were instantly converted into heat). Indeed high tempera-
34 tures are needed to obtain a spectrum such as the one ob-
35 served for VW Hyi. The aim of our paper is to study the struc-
36 ture of the boundary layer under heat conduction. We discuss
37 what might cause low heat conduction that seems different from
38 heat conduction in other astrophysical situations. As the analy-
39 sis of thermal conduction in clusters of galaxies by Narayan and
40 Medvedev (2001) shows, a low conductivity would point to a
41 non-chaotic magnetic field.

42 In Sect. 2 we describe the observations we use for our com-
43 parison. In Sect. 3 we briefly discuss the physics entering our
44 structure computations as well as the boundary conditions at the
45 bottom and the top of the boundary layer. We compare different
46 models in Sect. 4. In Sect. 5. the results of the structure compu-
47 tations are presented, in Sect. 6 the evaluated spectra. We argue
48 that the spectra of other dwarf novae also indicate low thermal
49 conductivity in these systems. We discuss the presence of low
50 or high thermal conductivity indicated in different astrophysi-
51 cal sources as clusters of galaxies and the intercluster medium
52 (Sect. 7). The low conductivity found here possibly indicates an
53 important role of the magnetic field in the boundary layer accre-
54 tion process. Our conclusions follow in Sect. 8.

55 2. X-ray observations

56 For the comparison of our theoretical spectra with observation
57 we use the *XMM-Newton* spectrum (Jansen 2001) of VW Hyi
58 obtained with the European Photon Imaging Camera (EPIC)
59 (Strüder et al. 2001). This system was observed with the EPIC-
60 pn in full-frame mode on 2001 October 19 for 16.1 ks, from
61 06:10:05 to 10:38:34, in quiescent state, 22 days after a nor-
62 mal outburst and 23 days before the next outburst (which was a

superoutburst). The spectrum was extracted using SAS version. 63
The observed spectrum is shown in Fig. 5. The same data for 64
VW Hyi have also been used by Pandel et al. (2003) and were 65
included in the work by Pandel et al. (2005). 66

67 3. The boundary layer structure

68 We describe the accretion process through the boundary layer
69 around the white dwarf mainly as presented in an earlier work
70 (Liu et al. 1995). Passing through a turbulent region, the ac-
71 creting matter totally loses its angular momentum, becomes sub-
72 sonic and forms a layer around the white dwarf. We assume that
73 the density is higher towards the equatorial plane, so that ac-
74 cretion occurs onto a belt around the white dwarf. We assume
75 that its area is about half of the full stellar surface area. We take
76 spherical coordinates with r the distance to the white dwarf cen-
77 ter, r_* the white dwarf radius, and $S = r_* - r$ the height above
78 the white dwarf surface (negative sign). The downward directed
79 thermal conductive flux is

$$80 F_c = -\kappa_0 T^{5/2} \frac{dT}{dS} \quad (1)$$

81 with T temperature, κ_0 thermal conductivity coefficient, taken as
82 the standard value $\kappa_{\text{Sp}} = 10^{-6} \text{ g cm}/(\text{s}^3(\text{K})^{7/2})$ (Spitzer 1962).
83 Heat conduction is an important feature in the model, different
84 to a cooling flow model. We evaluate the structure for different
85 values of the thermal conductivity κ_0 , $1/5$, $1/25$ and $1/100$ of κ_{Sp} .
86 Mass conservation gives

$$87 \dot{M} = 2\pi r^2 \rho v = \text{const.} \quad (2)$$

88 with \dot{M} accretion rate, ρ density and v flow velocity (positive if
89 downward directed). Euler’s equation in the stationary case is

$$90 v \frac{dv}{dS} + \frac{1}{\rho} \frac{dP}{dS} - \frac{GM_*}{r^2} = 0 \quad (3)$$

91 with P pressure, G gravitational constant, M_* mass of the white
92 dwarf. Energy conservation gives

$$93 \frac{1}{r^2} \frac{d}{dS} \left[\frac{\dot{M}}{2\pi} \left(\frac{1}{2} v^2 + \frac{GM_*}{r_*} - \frac{GM_*}{r} + \frac{\gamma}{\gamma-1} \frac{P}{\rho} \right) + r^2 F_c \right] = \quad (4)$$

$$94 -\Lambda(T) n_e n$$

95 with $\gamma = \frac{5}{3}$ the ratio of specific heats for the fully ionized gas,
96 atom and electron densities n , n_e and $\Lambda(T)$ the radiative loss
97 function for solar abundance (Sutherland & Dopita 1993). In
98 our highly subsonic solutions the kinetic energy term is negli-
99 gibly small. We have normalized the gravitational potential en-
100 ergy to zero at the white dwarf surface. (Following Shmeleva &
101 Syrovatskii (1973)), we had added a source term to account for
102 the finite surface temperature of the white dwarf, see Liu et al.
103 (1995). We solve these equations together with the equation of

104 We assume that before radiative losses of the settling gas be-
105 come important, the accretion flow has already lost its angular
106 momentum, with which it started from the corona at the disk
107 truncation radius, and that the rotational energy has been dissi-
108 pated into heat. The maximum energy which this flow can bring
109 with it is then the gravitational energy between the disk trunca-
110 tion radius and the white dwarf surface where the former term
111 can be neglected if the truncation radius is many white dwarf
112 radii away. Support for our neglect comes from the boundary
113 layer rotation velocities derived by Pandel et al. (2005) for the

1 dwarf novae in their sample, found to be considerably smaller
2 than the Keplerian velocity near the white dwarf.

3 Our boundary conditions are the following. The lower
4 boundary is located at the white dwarf surface. The temperature
5 is taken equal to the black body temperature arising from the
6 irradiation of the surface by the downward directed half of the
7 radiative energy release. For the location of the upper boundary
8 we take a height above the white dwarf surface above which the
9 radiative loss is negligible. At this height we require that the total
10 energy flow, i.e. the sum of advective, gravitational and thermal
11 conductive flow, equals the total available accretion energy flow.
12 These energies are

$$\dot{E}_{\text{conductive}} = 2\pi r^2 F_c \quad (5)$$

$$\dot{E}_{\text{advective}} = \dot{M} \frac{\gamma}{\gamma - 1} \frac{\mathfrak{K}}{\mu} T \quad (6)$$

$$\dot{E}_{\text{gravitational}} = \dot{M} \frac{GM}{r_*} \left(\frac{1}{r_*} - \frac{1}{r} \right) \quad (7)$$

13 with \mathfrak{K} gas constant and μ molecular weight (taken as 0.6).

14 This boundary condition neglects outward conductive heat
15 losses at large radii where the temperature drops outwards. Such
16 losses have been estimated to be small in Liu et al. (1995) where
17 they amount, for full Spitzer conductivity, to the order of mag-
18 nitude of the evaporation energies at large radii. (Real tempera-
19 tures would come out slightly lower than with this neglect.) After
20 taking the mass accretion rate that corresponds to the observed
21 flux, our model contains no free parameter except the assumed
22 value of thermal conductivity, which we want to test.

23 4. Comparison of different models

24 In an isobaric cooling flow (Mushotzky & Szymkowiak 1988)
25 the emission measure for each temperature decrement is deter-
26 mined by the time it takes the matter to radiatively cool down to
27 the next temperature shell. No thermal conductivity is included.
28 To simulate the observed spectrum a mass flow rate that corre-
29 sponds to the observed flux is taken, in addition as a free param-
30 eter a maximal temperature is chosen to fit the observations.

31 Narayan & Popham (1993) investigated the structure of thin
32 accretion disks around a central white dwarf with emphasis on
33 a self-consistent description of the boundary layer. The decrease
34 of rotation from the Keplerian value at the upper boundary to
35 the value at the stellar surface as well as friction is taken into ac-
36 count. For low rates as appropriate for the dwarf nova systems in
37 quiescence they found an optically thin very hot boundary layer.
38 Heat is transported advectively into the optically thick layers of
39 the white dwarf from where it is radiated as X-rays. These inves-
40 tigation are carried out only for accretion rates 10 times higher
41 or even more than in our VW Hyi analysis.

42 The solutions based on a hot settling flow by Medvedev &
43 Narayan (2001); Medvedev & Menou (2002) also include the
44 rotational energy of the accreting gas, so that the white dwarf
45 rotation and the viscous nature of the flow are accounted for.
46 Mahasena & Osaki (1999) model the boundary layer structure
47 as determined by thermal conduction in the settling gas around
48 the white dwarf, similar to the ‘‘siphon-flow model’’ for a disk
49 corona (Meyer & Meyer-Hofmeister 1994), and also similar to
50 our white dwarf boundary modeling.

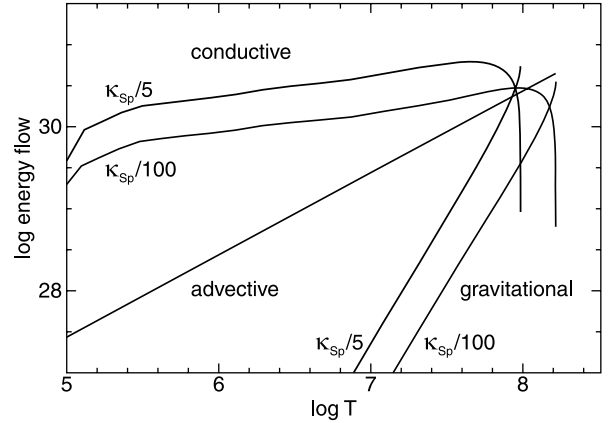


Fig. 1. Energy flux versus temperature for heat conductivity 1/5 and 1/100 of the Spitzer value. Note the higher temperature maximum, 1.6×10^8 K, for the lower conductivity value.

5. Results of computations

5.1. Energy flows in the boundary layer

51 We solve the system of differential equations given in the pre-
52 vious section, the same procedure as carried out for the earlier
53 investigation (Liu et al. 1995). For our comparison of theoret-
54 ical and observed spectra for VW Hyi we take $0.62 M_{\odot}$ for the
55 white dwarf mass and 8.3×10^8 cm for its radius. We do not
56 perform computations for different abundances since the aim of
57 our analysis is the study of the influence of thermal conduc-
58 tivity. The change of abundances allows better fits of the ob-
59 served spectrum. For a discussion of the abundances present in
60 VW Hyi see the discussion in Pandel et al. (2005). The free
61 parameter in our model is the mass accretion rate. We take
62 $\dot{M} = 1.25 \times 10^{-12} M_{\odot}/\text{yr}$ assuming that the matter is accreted on
63 an equatorial belt covering half of the white dwarf surface area.
64 Because we find that 100% the Spitzer value does not give an
65 acceptable agreement with the observations, we vary the value
66 of heat conductivity. In the following we show results for 1/100
67 and 1/25 and 1/5 of the standard Spitzer value.
68

69 In Fig. 1 we show the evaluated change of energy flows with
70 increasing height, that is increasing temperature for a heat con-
71 duction reduced to 1/5 and 1/100 of the standard value. The up-
72 per boundary location (according to the requirements discussed in
73 the last section) is at different heights above the white dwarf
74 surface, at 6.8×10^8 cm in the first case and 1.8×10^9 cm in the
75 second case. For the lower conductivity the advective energy is
76 dominant at high temperature. The most important difference is
77 the maximum temperature reached. This has a strong influence
78 on the resulting emission measures (and the spectrum) as will
79 be shown later. In our model the maximum temperature is a re-
80 sult of the structure computations. Note that in the cooling flow
81 model the maximal temperature is chosen to fit the spectrum.
82

5.2. Emission measures

83 In Fig. 2 differential emission measures (emission measures per
84 cm^2 surface area, per degree) [$\text{cm}^{-5} \text{K}^{-1}$] are shown for a heat
85 conductivity 1/5 and 1/100 of the standard Spitzer value. For
86 the higher value of heat conductivity the differential emission
87 measures are systematically higher, but with no contribution at
88 high temperature.
89

90 To obtain the radiation from the boundary layer, the differ-
91 ential emission measures have to be multiplied by the area from

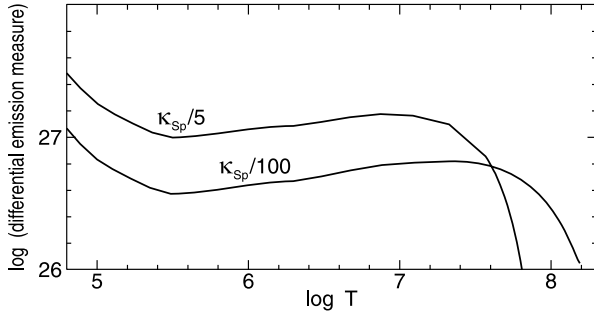


Fig. 2. Differential emission measures per surface area [$\text{cm}^{-5} \text{K}^{-1}$] for heat conductivity 1/5 and 1/100 of the standard Spitzer value.

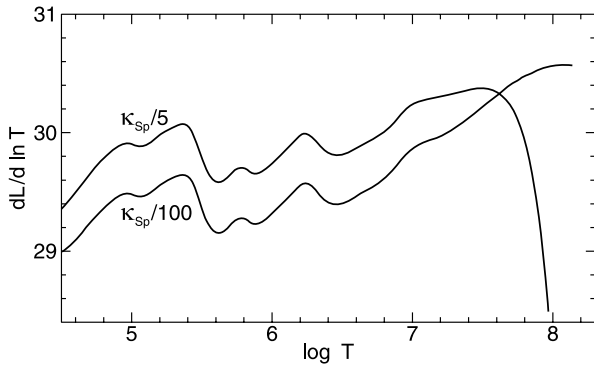


Fig. 3. Total emission per logarithmic temperature interval for heat conductivity 1/5 and 1/100 of the standard Spitzer value.

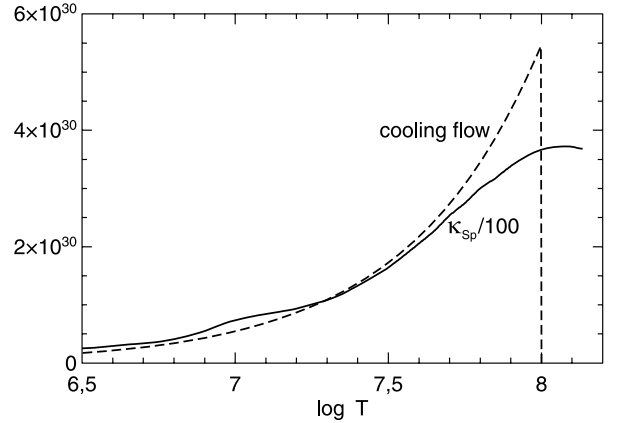


Fig. 4. Comparison of total emission per logarithmic temperature interval for a cooling flow model and our model for low conductivity.

ature chosen for the fit, $T_{\text{max}} = 9.5 \times 10^7$ K, so the emission is roughly compensated.

6. Spectra

We use the X-ray spectral fitting package XSPEC (version 11). We evaluated the spectra for the three sets of boundary layer structure computed for the conductivity 1/5, 1/25 and 1/100 of the standard Spitzer value. We show these spectra in Figs. 5a–c. The spectra document how the thermal conductivity determines the distribution of radiation over the energy range. A comparison of Fig. 3 shows how the different contributions to the radiation for high and low conductivity values determine the spectrum for temperatures around 10^7 and 10^8 . Below each spectrum the χ -statistics values are shown. Note the different scales in Figs. 5a–c. Only for the low conductivity do we find an acceptable agreement.

We have not tried to obtain the best fit for a variation of the mass accretion rate, nor for changes of the abundances, and we have not analyzed spectral lines, as was done in previous work (Pandel et al. 2003; Perna et al. 2003; Pandel et al. 2005). The aim of our investigation is to study the influence of the heat conductivity.

We compare the accretion rate roughly found from our modeling, $1.25 \times 10^{-12} M_{\odot}/\text{yr}$, with the rates derived in other investigations. Pandel et al. (2003) found $5 \times 10^{-12} M_{\odot}/\text{yr}$ and Pandel et al. (2005) $3.7 \times 10^{-12} M_{\odot}/\text{yr}$, for fits to the same data. Previous observations for VW Hyi lead to an estimate of $3 \times 10^{-12} M_{\odot}/\text{yr}$ for the accretion rate in late quiescence (BeppoSAX observations by Hartmann et al. 1999); similar results were gained from earlier observations (EXOSAT and ROSAT observations by van der Woerd et al. 1987; Belloni et al. 1991). From theoretical arguments one would expect that the X-ray flux changes during the quiescent interval in the outburst cycle. One would expect an increase of the rate in quiescence due to the increasing amount of matter accumulated in the disk and the increasing mass flow rate (Meyer-Hofmeister & Meyer 1988).

We note that the observations also include the radiation from the accretion disk. In earlier work we compared the amount of X-rays from the accretion disk and from the white dwarf boundary layer for VW Hyi (Meyer et al. 1996, Fig. 1) and found that the distribution of radiation over the energies is similar in both cases, but the total contribution from the boundary layer is much smaller. This means that the shape of the spectrum of the white dwarf boundary layer should not be essentially changed by an

1 which the radiation comes, the temperature T and the cooling
 2 function $\Lambda(T)$. The surface area is the spherical shell around
 3 the white dwarf at the height with temperature T . Since all the
 4 boundary layer is close to the white dwarf this flaring effect in
 5 the geometry only occurs at the highest temperatures. This prod-
 6 uct, the evaluated contributions to the luminosity from differ-
 7 ent temperature regions, is shown in Fig. 3. The departure from
 8 smooth lines is due to the non-smooth dependence of the cooling
 9 function on temperature. With this display of luminosity distri-
 10 butions it becomes clear that different contributions arise from
 11 the structure at high temperatures. And, as shown in the next
 12 section, agreement with the observed spectrum for VW Hyi can
 13 only be gained with the high temperature contributions which
 14 result from the low conductivity.

15 The emission measures of a cooling flow model are (see
 16 Pandel et al. 2005, taken from Mushotzky & Szymkowiak 1988)

$$17 \quad \frac{dEM}{dT} = \frac{5}{2} \frac{\mathfrak{R}}{\mu} \dot{M} \frac{n^2}{\varepsilon(T, n)} \quad (8)$$

18 with $\varepsilon(T, n)$ the total emissivity per volume. The total emission
 19 per logarithmic temperature then becomes $dEM/dT \Lambda(T) T =$
 20 $\frac{5}{2} \frac{\mathfrak{R}}{\mu} \dot{M} T$. Pandel et al. (2005) modified the cooling flow model
 21 emission measures adding a factor $(T/T_{\text{max}})^{\alpha}$, with $\alpha = -0.05$
 22 for VW Hyi to improve the fit of the spectrum, and derived an ac-
 23 cretion rate of $3.7 \times 10^{-12} M_{\odot}/\text{yr}$. We use $1.25 \times 10^{-12} M_{\odot}/\text{yr}$ for
 24 our calculation, the matter accreting onto half the white dwarf
 25 surface. To compare the cooling flow radiation with our results
 26 for low conductivity we have multiplied these cooling flow emis-
 27 sion measures (without α modification) by a factor of 0.676
 28 (=ratio of accretion rates, our rate doubled) to account for the
 29 different accretion rates and accretion areas. The result is shown
 30 in Fig. 4. The contributions from the cooling flow model lie
 31 above those from our model, but end at the maximum temper-

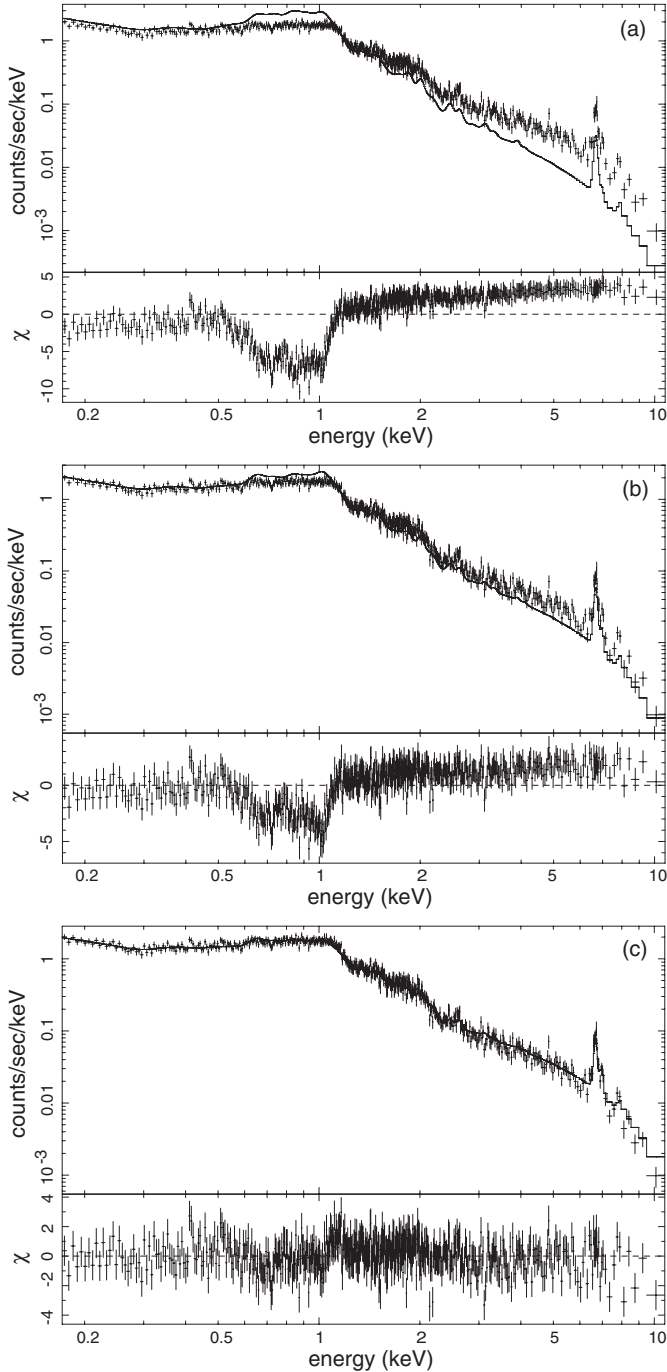


Fig. 5. Comparison of XMM-Newton EPIC spectra for VW Hyi in quiescence with model spectra evaluated for an accretion rate of $\dot{M} = 1.25 \times 10^{-12} M_{\odot}/\text{yr}$ and for different thermal conductivity: **a)** $1/5\kappa_{\text{Sp}}$, **b)** $1/25\kappa_{\text{Sp}}$ and **c)** $1/100\kappa_{\text{Sp}}$.

1 additional contribution of disk X-ray emission and we can interpret the observed spectrum as the spectrum of the boundary layer.
2
3

4 7. Discussion

5 7.1. Spectra from different models

6 The first comparisons with emission line spectra from the new
7 X-ray telescopes were carried out for other dwarf novae, not
8 VW Hyi. Ramsay et al. (2001b) presented a spectrum of OY Car

(in quiescence) obtained during the performance phase of the
9 *XMM-Newton* mission (Ramsay et al. 2001a). They found that
10 the spectrum was best fitted by a three temperature MEKAL
11 thermal plasma model with a partial covering absorber. Mukai
12 et al. (2003) discussed *Chandra* HETG spectra of seven CVs
13 and found for the non-magnetic systems EX Hya, V603 Aql,
14 U Gem and SS Cyg that they are remarkably well fit by a cool-
15 ing flow model.
16

17 Perna et al. (2003) performed the first comparison with theo-
18 retical spectra, evaluated for the models by different authors,
19 which were available at that time. Their very detailed analysis
20 for WX Hyi in quiescence includes line effects, not included in
21 our analysis. The results were: (1) for the cooling flow model
22 they found it accounts reasonably well for the continuum of
23 WX Hyi and the line strength in the short-wavelength region,
24 but under-predicts the emission at long wavelength; (2) for the
25 model of Narayan & Popham (1993) they found that the in-
26 crease of density in the outer regions results in substantially
27 more emission in O VII and O VIII lines than in a cooling
28 flow. The agreement between observed and predicted low tem-
29 perature lines is reasonable and could be due to the assumed
30 bremsstrahlung cooling; (3) for the coronal siphon flow model of
31 Meyer & Meyer-Hofmeister (1994), emission measures derived
32 for the transition layer between corona and disk were taken.
33 However the more important emission measures for the accre-
34 tion layer on the white dwarf were given in Liu et al. (1995); (4)
35 the spectra from the X-ray emitting corona model of Mahasena
36 & Osaki (1999), for the assumed low accretion rate, plausible
37 for WX Hyi, show a too soft continuum and too strong emission
38 lines. But the fit with higher accretion rate for U Gem was bet-
39 ter; (5) for the hot settling flow solutions (Narayan & Medvedev;
40 Medvedev & Menou 2002) the accretion rate was adjusted to a
41 value to reproduce the observed X-ray luminosity, but the X-ray
42 line emission seems greatly over-predicted.

43 For VW Hyi a first spectral analysis was performed by
44 Pandel et al. (2003). They found the best agreement between
45 observations and computed spectrum for a CEMEKL model,
46 slightly better than for a three-temperature model, and also a
47 good fit for the MKCFLOW cooling flow model. The authors
48 pointed out a remarkable qualitative agreement with the model
49 of Narayan & Popham (1993). In the spectral analysis of Pandel
50 et al. (2005) based on *XMM-Newton* data, including VW Hyi, it
51 was found that, in general, the X-ray emission originates from a
52 hot, optically thin multi-temperature plasma with a temperature
53 distribution in close agreement with an isobaric cooling flow.

54 These discussions of spectra resulting from different models
55 only allow the conclusion that spectra of a cooling flow model or
56 a combination of a few MEKAL one-temperature models give a
57 good fit. To really test the other boundary layer models, detailed
58 calculations for a chosen dwarf nova system would have to be
59 carried out (as done for our model) to compare the model with
60 the observed spectrum.

61 7.2. Spectra of other dwarf novae

62 The investigation of ten dwarf novae by Pandel et al. (2005) al-
63 lows a comparison of the results for the different systems. From
64 Fig. 1 in their work showing all spectra together, the spectra of
65 the eight dwarf novae in quiescence look qualitatively similar,
66 except that of OY Car (the lower flux at low energies attributed to
67 intrinsic absorption) and EI UMa (the harder spectral slope (in-
68 terpreted as characteristic for the intermediate polar objects). An
69 important result is the maximal temperature found for these sys-
70 tems. For seven of these systems (U Gem omitted) the maximal

1 temperatures found from the fits lie in the range from 9.5×10^7 K
 2 (VW Hyi) to 3×10^8 K (WX Hyi). That means to fit the spectra
 3 of the other systems we also would have to assume a low heat
 4 conductivity.

5 7.3. High and low thermal conductivity

6 There is evidence for both high and low thermal conductivity in
 7 different astrophysical situations.

8 On one hand, observations indicate that thermal conduction
 9 across the temperature jumps of cold fronts in clusters of galax-
 10 ies (e.g. Abell 2142 and Abell 3667) is far below the Spitzer
 11 value (Markevitch et al. 2000; Etori & Fabian 2000; Vikhlinin
 12 et al. 2001). This is interpreted as resulting from gas motion
 13 on both sides of the interface that produces a magnetic field
 14 stretched parallel to the interface (Vikhlinin et al. 2001). SPH
 15 calculations relate the width of the cold front to the value of the
 16 thermal conductivity and support this explanation, yielding a re-
 17 duction to the percent level of the Spitzer value (Asai et al. 2004;
 18 2007; Xiang et al. 2007).

19 On the other hand, modeling the temperature gradients of
 20 cooling flows in clusters of galaxies Zakamska & Narayan
 21 (2003); Ghizzardi et al. (2004); Voigt & Fabian (2004) found
 22 evidence for thermal conduction of about 30 up to near 100%
 23 of the Spitzer value. Narayan & Medvedev (2001) suggested
 24 that such high values can result in tangled and chaotic mag-
 25 netic fields (Rechester & Rosenbluth 1978; Chandran & Cowley
 26 1998) if the field is chaotic over a wide range of length scales
 27 (factors of 100 or more) as might happen in strong MHD turbu-
 28 lence (Goldreich & Sridhar 1995). In contrast, low thermal con-
 29 ductivity should result for weak MHD turbulence (effectively a
 30 superposition of Alfvén waves).

31 High thermal conductivity, near the Spitzer value, appears
 32 also to be present in coronal boundary layers above accretion
 33 disks. In X-ray binaries, features like spectral state transitions
 34 and hysteresis can be well modeled in the framework of disk
 35 evaporation (Meyer & Meyer-Hofmeister 1994; Meyer et al.
 36 2000) that takes the exchange of mass and energy between disk
 37 and corona into account. In such models the flow of mass from
 38 the disk into the corona depends significantly on the value of
 39 the thermal conductivity (Meyer-Hofmeister & Meyer 2006).
 40 Quantitative agreement with observations results for high values
 41 of the thermal conductivity.

42 7.4. High conductivity a result of disk dynamo action?

43 The high conductivity found in the cases discussed above differs
 44 remarkably from the low conductivity found here, for an appar-
 45 ently similar accretion process, here from a hot corona to the
 46 cool white dwarf surface. Narayan & Medvedev's (2001) sug-
 47 gession implies strong MHD turbulence in the layers between
 48 corona and disk but not in the corresponding layers between
 49 corona and white dwarf surface. Stable layering of the cooling
 50 gas in the strong gravity of the white dwarf might suppress tur-
 51 bulence in the white dwarf case.

52 High thermal conductivity in the coronal transition layers of
 53 accretion disks could also result from magnetic fields generated
 54 through dynamo action in the accretion disks. These fields at-
 55 tain energy densities that are a fraction of the disk internal pres-
 56 sure but reach out into the low density atmosphere of the disk
 57 where they become dominant over the gas pressure (Hirose et al.
 58 2006). One also notes that magnetic diffusion in the accretion
 59 disk transports magnetic power from small scales, of the order

of the disk scale height (on which the fields are generated) to
 large scales, up to the size of the local disk radius (Brandenburg
 et al. 1995). Large scale unipolar fields reach farther than a few
 scale heights of the disk into the corona where they will merge
 with coronal magnetic fields. Continuous reconnection could re-
 sult in a fairly direct thermal path along magnetic field lines from
 corona to disk and provide high thermal conductivity in the con-
 ductively heated and radiatively cooling transition layer.

57 7.5. Magnetic fields advected in white dwarf accretion

58 The very low thermal conductivity in white dwarf accretion
 59 raises an important question. The high thermal conductivity
 60 *along* magnetic field lines suggests thermal insulation in these
 61 accreting layers by a nearly horizontal magnetic field. Is this a
 62 natural outcome of accretion from a hot ADAF-like coronal flow
 63 with turbulent magnetic fields? We show that this might point to
 64 a very different accretion geometry than that commonly consid-
 65 ered.

66 The mean magnetic energy density in accretion disks ob-
 67 tained in magneto-hydrodynamic simulations typically is a frac-
 68 tion of the gas energy density, e.g. one quarter (Hirose et al.
 69 2006; Sharma et al. 2006, the latter for collision-free plasma).
 70 Due to shearing Kepler motion the azimuthal component of the
 71 mean magnetic field is larger than the poloidal components, e.g.
 72 by a factor of 6. Treating the ADAF as a thick accretion disk, we
 73 now can estimate the strength of the azimuthal magnetic field
 74 in the gas approaching the white dwarf. This gas and its mag-
 75 netic field become highly compressed as they settle in the strong
 76 gravity on the white dwarf surface. The compression ratio can be
 77 estimated by comparing the density in the ADAF near the white
 78 dwarf with the density in the cooling layer. Using the cooling
 79 layer solution for VW Hyi and the ADAF solution of Narayan
 80 et al. (1998) (for $\alpha = 0.3$ and the same mass flow rate), one
 81 obtains a factor $10^{1.9}$ by which the density is increased.

82 With flux conservation, the toroidal component of the mag-
 83 netic field increases by the same factor while the radial com-
 84 ponent only increases by a geometrical factor, the ratio of the
 85 ADAF surface to the white dwarf surface, a factor of 4 if the
 86 ADAF ends at a height of one stellar radius above the white
 87 dwarf surface. Since we are interested only in an approximate
 88 order of magnitude the exact numbers are not important. Also,
 89 the possible weakening of the toroidal flux by compression of
 90 oppositely directed field lines and annihilation may be neglected.
 91 (The mass that ends up in the settling layer has previously occu-
 92 pied an ADAF region of the size of a radius, the typical size of
 93 magnetic fields created by a coronal dynamo.)

94 This simple exercise yields a ratio between the magnetic
 95 field components parallel and perpendicular to the surface of
 96 the white dwarf of the order of 100, that would result in a cor-
 97 responding reduction of the radial thermal conductivity by the
 98 same factor. However, the same estimate yields a magnetic field
 99 strength whose pressure far exceeds the gas pressure in the cool-
 100 ing region, by about a factor of 100. This invalidates the assump-
 101 tion of a plane gas pressure supported cooling flow, with inter-
 102 esting consequences.

103 7.6. Cooling gas suspended in magnetic fields?

104 Cooling gas supported against gravity by gas pressure and
 105 the magnetic pressure of a horizontal magnetic field becomes
 106 strongly unstable to the Parker instability when the magnetic
 107 pressure becomes a significant part of the total pressure: an al-
 108

ternating vertical up-and-down displacement of an initially horizontal flux tube creates peaks and troughs so that matter can flow along the flux tube to collect in the troughs and evacuate the peaks. The troughs become heavier than their surroundings and sink down, the peaks become buoyant and rise. If the magnetic tensions become dominant, as in our case, this will end up in narrow filaments of matter magnetically suspended above the white dwarf surface, reminiscent of solar filaments of cool chromospheric gas magnetically suspended in the corona. The transport of angular momentum of the accreting gas, of course, needs further consideration. We only note that the magnetic field configuration might lend itself to effective removal of angular momentum.

Thus from the simple advection of coronal/ADAF magnetic fields a spatially intermittent accretion flow will arise, possibly involving the formation of accretion spots. It is interesting that this very different geometry preserves the thermal insulation of the cooling gas: gas of different temperature resides in different flux tubes. Would this situation also lead to cooling under constant pressure as the analysis of observed spectra indicates? The gas pressure in the flux tubes is the weight of the column density, and as the column density remains constant on cooling, so does the pressure. Thus our good fits to the observed spectra could be the natural signature of accretion from a hot magnetized ADAF on non-magnetic white dwarfs in the quiescent stage of dwarf novae cycles.

8. Conclusions

We have calculated the structure of the boundary layer that forms at the surface of non-magnetic white dwarfs on accretion from a hot corona in quiescent dwarf nova systems. Our calculated spectra significantly depend on the value of the thermal conductivity. Comparing our results with observed spectra for VW Hydri we find good agreement for very low values of the conductivity, of the order of 1% of the Spitzer value for ionized gases. For higher values too much energy is drained from the hottest layers and radiated at cooler temperatures to give a satisfactory fit.

This suggests thermal insulation of layers of different temperature from each other by magnetic fields. A discussion of high and low conductivity cases in various circumstances leads us to the suggestion of spatially intermittent accretion in magnetic fields, preserving the low thermal conductivity isobaric cooling that our spectral fits require.

Acknowledgements. F. K. Liu acknowledges the support of the National Natural Science Foundation of China (No. 10573001) and thanks MPA for hospitality.

References

- Asai, N., Fukuda, N., & Matsumoto, R. 2004, *ApJ*, 606, 105
 Asai, N., Fukuda, N., & Matsumoto, R. 2007, *ApJ*, 663, 816
 Balsara, D. S., Fisker, J. L., Godon, P., & Sion, E. M. 2007, [*astro-ph arXiv:0705.2582*], *ApJ*, submitted
 Belloni, T., Verbunt, F., Beuermann, K., et al. 1991, *A&A*, 246, L44
 Brandenburg, A., Nordlund, A., Stein, R. F., et al. 1995, *ApJ*, 446, 741
 Etorri, S., & Fabian, A. C. 2000, *MNRAS*, 317, L57
 Chandran, B. D. G., & Cowley, S. C. 1998, *Phys. Rev. Lett.* 80, 3077
 Ghizzardi, S., Molendi, S., Fabio, P. M., et al. 2004, *ApJ*, 609, 638
 Goldreich, P., & Sridhar, S. 1995, *ApJ*, 438, 763
 Hartmann, H. W., Wheatley, P. J., Heise, J., et al. 1999, *A&A*, 349, 588
 Hirose, S., Krolik, J. H., & Stone, J. M. 2006, *ApJ*, 640, 901
 Jansen, F., Lumb, D., Altieri, B., et al. 2001, *A&A*, 365, L1
 Liu, F.K., Meyer, F., & Meyer-Hofmeister, E. 1995, *A&A*, 300, 823
 Liu, B.F., Meyer, F., & Meyer-Hofmeister, E. 1997, *A&A*, 328, 247
 Mahasena, P., & Osaki, Y. 1999, *PASJ*, 51, 45
 Markevitch, M., Ponman, T. J., Nulsen, P. E. J., et al. 2000, *ApJ*, 541, 542
 Medvedev, M. V., & Menou, K. 2002, *ApJ*, 565, L39
 Medvedev, M. V., & Narayan, R. 2001, *ApJ*, 554, 1255
 Meyer, F., & Meyer-Hofmeister 1984, *A&A* 132, 143
 Meyer, F., & Meyer-Hofmeister, E., & Liu, F.K. 1996 in *Röntgenstrahlung from the Universe*, ed. Zimmermann, H.U., Trümper, J., Yorke, H., MPE Report 263, 163
 Meyer, F., & Meyer-Hofmeister, E. 1994, *A&A*, 288, 175
 Meyer, F., Liu, B. F., & Meyer-Hofmeister, E. 2000, *A&A*, 361, 175
 Meyer-Hofmeister, E., & Meyer, F. 1988, *A&A*, 194, 135
 Meyer-Hofmeister, E., & Meyer, F. 2006, *A&A*, 449, 443
 Mukai, K., Kinkhabwala, A., Peterson, J. R., et al. 2003, *ApJ*, 586, L77
 Mushotzky, R. F., & Szymkowiak, A. E. 1988, in *Cooling Flows in Clusters and Galaxies*, ed. A. C. Fabian (Kluwer Academic Publishers), 53
 Narayan, R., & Popham, R. 1993, *Nature*, 362, 820
 Narayan, R., Mahadevan, & R., Quataert, E. 1998, in *The Theory of Black Hole Accretion Discs*, ed. M. A. Abramowicz et al. (Cambridge Univ. Press), 48
 Narayan, R., & Medvedev, M. V. 2001, *ApJ*, 562, L129
 Pandel, D., Cordova, F. A., & Howell, S. B. 2003, *MNRAS*, 346, 1231
 Pandel, D., Cordova, F. A., Mason, K. O., et al. 2005, *ApJ*, 626, 396
 Perna, R., McDowell, J., & Menou, K. 2003, *ApJ*, 598, 545
 Ramsay, G., Órdova, J., Mason, K., et al. 2001b, *A&A*, 365, L294
 Ramsay, G., Poole, T., Mason, K., et al. 2001a, *A&A*, 365, L288
 Rechester, A. B., & Rosenbluth, M. N. 1978, *Phys. Rev. Lett.*, 40, 38
 Sasonov, S., Revnitsev, M., Gilfanov, M., et al. 2006, *A&A*, 450, 117
 Sharma, P., Hammer, W. Quataert, E., et al. 2006, *ApJ*, 637, 952
 Shmeleva, O. P., & Syrovatskii, S. I. 1973, *Sol. Phys.* 33, 341
 Spitzer, L. 1962, *Physics of Fully Ionized Gases*, 2nd edition, (New York, London: Interscience Publishers)
 Strüder, L., Briel, U., Dennerl, K., et al. 2001, *A&A*, 365, L18
 Sutherland, R. S., & Dopita, M. A. 1993, *ApJ*, 88, 253
 Turner, M. J. L., Abbey, A., & Arnaud, M. 2001, *A&A*, 365, L27
 van der Woerd, H., & Heise, J. 1987, *MNRAS*, 225, 141
 Vikhlinin, A., Markevitch, M., & Murray, S. S. 2001, *ApJ*, 551, 160
 Voigt, L. M., & Fabian, A. C. 2004, *MNRAS*, 347, 1130
 Xiang, F., Churazov, E., Dolag, K. et al. 2007, *MNRAS*, 379, 1325
 Zakamska, N. L., & Narayan, R. 2003, *ApJ*, 582, 162